ICMLS Cellular and Molecular Life Sciences

Research Article

In pre-sterol carrier protein 2 (SCP2) in solution the leader peptide 1–20 is flexibly disordered, and residues 21–143 adopt the same globular fold as in mature SCP2

F. E. Weber[a], J. H. Dyer[a], F. López García[b], M. Werder[a], T. Szyperski[b], K. Wüthrich[b] and H. Hauser[a],*

[a]Institut für Biochemie, Eidgenössische Technische Hochschule – Zentrum, CH-8092 Zürich (Switzerland), Fax +41 1 632 3145
[b]Institut für Molekularbiologie und Biophysik, Eidgenössische Technische Hochschule – Hönggerberg, CH-8093 Zürich (Switzerland)

Abstract. The preform of the rabbit sterol carrier protein 2 (pre-rSCP2) was cloned, the uniformly ^{15}N-labelled protein expressed in *Escherichia coli* and studied by three-dimensional ^{15}N-resolved nuclear magnetic resonance spectroscopy. In spite of its low solubility in aqueous solution of only ~0.3 mM, sequential ^{15}N and ^{1}H backbone resonance assignments were obtained for 105 out of the 143 residues. From comparison of the sequential and medium-range nuclear Overhauser effects (NOEs) in the two proteins, all regular secondary structures previously determined in mature human SCP2 (hSCP2) [Szyperski et al. (1993) FEBS Lett. **335**: 18–26] were also identified in pre-rSCP2. Near-identity of the backbone ^{15}N and ^{1}H chemical shifts and 1:1 correspondence of 24 long-range NOEs to backbone amide groups in the two proteins show that the residues 21–143 adopt the same globular fold in pre-rSCP2 and mature hSCP2. The N-terminal 20-residue leader peptide of pre-rSCP2 is flexibly disordered in solution and does not observably affect the conformation of the polypeptide segment 21–143.

Twenty years have gone by since sterol carrier protein 2 (SCP2) was first characterized as a nonspecific lipid transfer protein of the rat liver [1], but its physiological function still remains largely unknown. Its occurrence in brain, lung, spleen, intestine and kidney, and the highly conserved primary structures of the rat [2], human [3], mouse [4] and chicken [5] proteins strongly suggest an important role of this 13-kDa basic protein for intracellular lipid trafficking. Most insights into the physiological function of SCP2 have been obtained from in vitro studies of enzyme activation and ligand binding, and from the recent correlation of its tertiary fold as determined by nuclear magnetic resonance (NMR) spectroscopy with in vitro studies of deletion mutants [6]. Key roles of purified SCP2 could be demonstrated for the in vitro conversion of sterol inter-

---

* Corresponding author.

mediates to cholesterol [7, 8], and in the formation of bile acids [9] and steroid hormones [10–12]. In vitro studies have also shown that SCP2 is a fatty acyl-coenzyme A-binding protein [13], and site-directed mutagenesis and deletion analysis provided information about regions in the protein that are involved in lipid interactions [14]. Very recent studies using transfected cells provided additional insight into the physiological role of SCP2. Thus, overexpression of SCP2 in stably transfected rat hepatoma cells appears to be correlated with changes in the rate of cholesterol cycling and distribution [15], and antisense treatment of male Wistar rats suggests that SCP2 is involved in the transfer of newly synthesized cholesterol into the bile [16].

Studies involving the intracellular localization of SCP2 indicated that a C-terminal Ala-Lys-Leu targeting sequence appears to provide localization in peroxisomes [17]. This targeting would be consistent with immunocytochemical studies [18–20], although SCP2 was also detected in the endoplasmic reticulum and mitochondria. Moreover, it has been suggested that the 20-amino acid N-terminal leader sequence of pre-SCP2 serves as a mitochondrial targeting signal [21]. Interestingly, transfection of a complementary DNA (cDNA) encoding the 15-kDa pre-SCP2 but not the mature 13-kDa SCP2 into murine L-cell fibroblasts resulted in increased cholesterol uptake by these cells [22] and increased exogenous cholesterol esterification [23].

Our search for a membrane-associated form of SCP2 [20, 24, 25] led to the cloning of a rabbit 2.2-kbase cDNA encoding SCPX, which subsequently allowed us to express recombinant ^{15}N-labelled pre-rSCP2 in sufficient quantity for NMR studies. Analysis of three-dimensional (3D) ^{15}N-resolved [^{1}H,^{1}H]-NMR experiments recorded with a 0.3-mM aqueous solution of pre-rSCP2 and comparison with spectral data acquired with mature hSCP2 [6] enabled us to characterize the key conformational properties of the 20-residue leader peptide of pre-rSCP2, and an assessment of possible changes in the structure of residues 21–143 that might result from the N-terminal extension when compared with the mature protein.

Materials and methods

Materials. Egg phosphatidylcholine (PC) and egg phosphatidic acid were purchased from Lipid Products (South Nutfield, Surrey, UK), cholesterol (>99%) from Fluka (Buchs, Switzerland), [1α, 2α(n)-^{3}H]cholesterol (47 Ci/mmol) from Amersham (Amersham, UK) and bicinchoninic acid protein assay reagent from Pierce (Lausanne, Switzerland).

Isolation of RNA. RNA was isolated from frozen pulverized tissue of adult rabbit small intestine by the acid-guanidinium-thiocyanate method. Intestinal messenger RNA (mRNA) was extracted from enterocytes, which were scraped from the luminal side of washed intestine with a microscope slide and frozen directly in liquid nitrogen. For the isolation of mRNA, the PolyA-Tract mRNA isolation system from Promega (Madison, WI, USA) was used.

Construction and screening of a cDNA library from enterocytes. A directional cDNA library was made with poly(A)-enriched RNA from rabbit small-intestinal enterocytes using the Superscript cDNA cloning system of Life Technologies (Basel, Switzerland). In order to avoid recloning SCP2, the mRNA was size-fractionated by ultracentrifugation in a sucrose gradient. For the library we used only mRNA exceeding 2 kb. The library in the pSPORT vector contained about 1×10^6 independent clones with an average size of 2.6 kb. The library was screened by colony hybridization and by polymerase chain reaction (PCR). For the colony hybridization we used a nick-labelled rat SCP2 cDNA as probe (kindly provided by Dr. Karel Wirtz, State University of Utrecht, The Netherlands). The final wash was performed with 15 mM NaCl/1.7 mM sodium citrate, pH 7.0 (0.1 $\times$ SSC) at 65 °C. In PCR reactions a pSPORT-specific forward or reverse primer and a gene-specific primer were used. Four different gene-specific primers were deduced from a partial amino acid sequence of a 13-kDa lipid exchange protein purified from rabbit intestinal brush-border membrane vesicles [25]. DNA from the pSPORT library was purified and amplified by PCR using Gene-Amp reagents (Perkin Elmer Cetus) and 35 reaction cycles as follows: 94 °C, 80-s denaturation; 55–65 °C, 2-min annealing; 72 °C 3-min elongation. The final elongation step was performed at 72 °C for 10 min. The annealing of the last 20 cycles was at 55 °C. For the first 15 cycles five different declining annealing temperatures were employed for 3 cycles each. The reaction products were phenol-extracted, ethanol-precipitated and size-fractionated on a 1% agarose gel. After transfer to a nylon membrane, the gene-specific products were identified with the rat SCP2 cDNA probe or with end-labelled gene-specific oligonucleotides. The size of these products was determined by agarose gel electrophoresis using DNA standards.

Generation of the pre-rSCP2 and mature rSCP2 expression constructs. The pre-rSCP2 expression construct was generated using PCR and the rabbit 2.2-kb cDNA (SCPX) construct as the template. Primers were a cDNA-specific primer at the 5′ end of the known pre-rSCP2 and a vector-specific primer at the 3′ end. PCR conditions were as described above; the gel-purified product was cloned into a pGEM-T vector (Promega, Madison, WI, USA) and sequenced from both ends.

The full-length pre-rSCP2 was cloned into the pET20b expression vector, which was then used to transform *Escherichia coli* strain BL21 cells. The mature rSCP2 expression construct was generated by PCR using the pre-rSCP2 construct as a template and a mature SCP2-specific primer and a M13 vector-specific primer at the 5′ end and 3′ end, respectively.

DNA sequencing. cDNA inserts of clones from the library and of the pre-rSCP2 and mature rSCP2 constructs were sequenced by the dideoxynucleotide-chain-termination method using the Sequenase 2.0 kit (USB, Cleveland, OH). Custom-made primers (MWG-Biotech) and vector-specific primers were used for the sequencing of both strands. Nucleotide sequences were read with a digitized gel reader and transferred to the ETH computer system. The analysis of the sequences was done with the software package GCG (University of Wisconsin Genetics Computer Group).

E. coli BL-21 cell culture and recombinant protein expression. Pre-rSCP2 cDNA and mature rSCP2 cDNA were cloned into a pET20b vector and expressed in *E. coli* strain BL-21. Protein for NMR studies was purified from bacteria grown on an M9 minimal medium [26] with $(^{15}NH_4)_2SO_4$ as the sole nitrogen source. Expression of protein was induced by addition of isopropyl β-D-thiogalactopyranoside at optical density $(OD)_{600} = 0.7$. Bacteria were harvested by centrifugation 12–15 h after induction, washed once with buffer A (10 mM Tris-HCl, 2 mM EDTA, pH 8.0), and stored at -70 °C until use.

Protein purification. All purification steps were carried out at 4 °C. Both pre-rSCP2 and mature rSCP2 were purified as follows: cells were thawed and suspended in buffer B (10 mM Tris-HCl, 2 mM EDTA, 5 mM DTT, pH 8.0, complemented by Complete Protease Inhibitor cocktail (from Boeringer, Mannheim, Germany). Bacteria were lysed and DNA sheared by passage through a French pressure cell at 20,000 psi. The lysate was centrifuged for 20 min at 12,000 rpm (Centrikon T-2050 centrifuge with a TFT65 rotor), and the supernatant was applied to a DEAE-Sepharose column (Pharmacia, Uppsala, Sweden). The SCP2 eluted with buffer B in the flow-through was applied to an SP-Sepharose column (Pharmacia). After rinsing off unbound proteins with buffer C (10 mM Tris-HCl, 2 mM EDTA, 5 mM DTT, pH 7.0), bound SCP2 was eluted with 0.2 M NaCl in buffer C. Fractions containing SCP2 were applied to a Sephadex G-75 column and eluted with buffer D (15 mM sodium phosphate, 2.5 mM DTT, pH 6.0). Fractions containing SCP2 were concentrated in an Amicon chamber using a regenerated cellulose, low-binding filter from Millipore with a nominal molecular weight cutoff of 5000. The presence of SCP2 was monitored throughout the purification by assaying for cholesterol exchange activity as described in 'Results and discussion', and by detection on SDS-15% polyacrylamide gel electrophoresis (PAGE) gels.

NMR spectroscopy. For the NMR experiments 0.55 ml of a 0.3-mM solution of pre-rSCP2 in 90% H_2O/10% D_2O containing 15 mM KH_2PO_4 and 5 mM DTT, pH 6.0, were placed in a 5-mm NMR tube under argon. All NMR spectra were recorded at 28 °C on a Bruker AMX 600 spectrometer, and quadrature detection in the indirectly detected dimensions was obtained employing States-TPPI [27]. For the data processing and analysis we used the programs PROSA [28] and XEASY [29], respectively. A two-dimensional (2D) [^{15}N,^{1}H]-HSQC experiment [30] was recorded with 150×2048 complex points, $t_{1max}(^{15}N) = 84$ ms and $t_{2max}(^1H) = 200$ ms. A 3D ^{15}N-resolved [^{1}H,^{1}H]-total correlation spectroscopy (TOCSY) experiment [31, 32] with a mixing time of 50 ms and a 3D ^{15}N-resolved [^{1}H,^{1}H]-nuclear Overhauser effect spectroscopy (NOESY) experiment [31, 33] with a mixing time of 120 ms were recorded with $32 \times 120 \times 1024$ complex points [$t_{1max}(^1H) = 18$ ms, $t_{2max}(^{15}N) = 16$ ms, $t_{3max}(^1H) = 112$ ms] in about 3 days and 6 days, respectively. Prior to Fourier transformation the water signal was reduced by the technique of Marion et al. [34], the data sets were multiplied in all dimensions with phase-shifted sine-bell functions [35] and a baseline correction [36] was applied.

Results and discussion

cDNA cloning and computer analysis. Previous work by some of us [25] suggested that SCP2 might be involved in lipid uptake at the brush-border membrane. We were interested in the question whether or not a membrane-bound form of SCP2 exists. To tackle this question, we constructed a pSPORT cDNA library exceeding 2 kb with mRNA from rabbit small-intestinal enterocytes and screened the library with the rat SCP2 cDNA kindly provided by Dr. Karel Wirtz. In addition to this approach, we followed a PCR strategy using oligonucleotides that were derived from a partial amino acid sequence of a 13-kDa lipid exchange protein isolated from rabbit small-intestinal brush-border membrane [25]. Both approaches led to the cloning of the same cDNA. The full-length clone exhibits a continuous sequence of 2651 nucleotides with a single open reading frame starting at nucleotide 53. This open reading frame encodes a protein of 547 amino acids (59 kDa). At nucleotide 1694 a termination codon is followed by a 3′ nontranslated sequence of 957 bp. Searching the Swiss protein database showed that the deduced amino acid sequence is 89% homologous to the amino acid sequences of SCPX from rat, mouse and human. The pre-rSCP2 region is located at the C-terminus of SCPX,

```
rabbit   1    MGFPEAASSF RTHQIEAAPT SSAGDGFKAN LVFKEIEKKL EEEGEQFVKK
human                        V          S


rabbit  51    IGGIFAFKVK DGPGGKEATW VVDVKNGKGS VLPNSDKKAD CTITIADSDL
human                                                       M        F


rabbit 101    LALMTGKMNP QSAFFQGKLK ITGNMGLAMK LQNLQLQPGK AKL  143
human                                                    N
```

Figure 1. Alignment of the amino acid sequences of pre-rSCP2 and mature hSCP2 [3]. Only those amino acid residues which differ between the two sequences are indicated for hSCP2. The 20-residue N-terminal leader sequence is depicted in boldface.

and its 143 amino acids add up to a molecular mass of 15.3 kDa. As shown in figure 1, the amino acid sequences of pre-rSCP2 and mature rSCP2 are 97% identical to the human analogue. The amino acid sequence of rabbit small-intestinal SCPX reported here has been deposited in the GenBank database (accession no. AF051897).

Expression and purification of pre-rSCP2 and mature rSCP2. Recombinant pre-rSCP2 was purified as described under 'Methods'. The protein obtained after the gel filtration step was homogeneous by the following criteria: a single band was obtained when 10 μg of protein was run on SDS-15% PAGE and silver-stained. A single band was also obtained with the same amount

of protein upon isoelectric focusing using silver staining. The latter result rules out the presence of isoforms of pre-SCP2 differing in electric charge. SDS-15% PAGE and Western blotting of recombinant pre-rSCP2 and mature rSCP2 purified as described in 'Methods' yielded single bands in distinctly different positions corresponding to apparent molecular masses of 16 and 14 kDa, respectively (fig. 2). The recombinant pre-rSCP2 was found to be active in cholesterol exchange
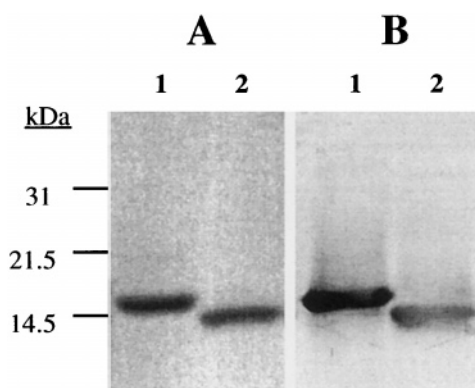

Figure 2. SDS-15% PAGE patterns (A) and immunoblots (B) of recombinant pre-rSCP2 (lanes 1) and mature rSCP2 (lanes 2). SDS-PAGE was carried out using the Mini-Protean II dual slab cell from Bio-Rad according to the Bio-Rad instruction manual. Proteins were visualized by Coomassie blue staining. Bio-Rad low-range protein standards were used as markers, and apparent molecular masses of these proteins in kDa are indicated on the left. Immunoblotting was carried out as described in ref. 25. For immunostaining of pre-rSCP2 and mature rSCP2 the polyclonal sheep antibody raised against pre-rSCP2 was used as the primary antibody. As the secondary antibody an alkaline phosphatase-conjugated rabbit anti-sheep antibody was used.

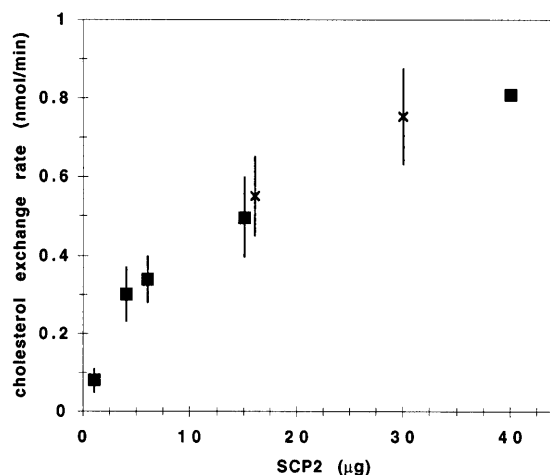Figure 3. Rate of cholesterol exchange between two populations of SUV in the presence of increasing quantities of recombinant pre-rSCP2 and mature rSCP2. Egg PC SUV containing 15 mol% egg phosphatidic acid, 20 mol% cholesterol and a trace amount of [^{3}H]cholesterol dispersed in 0.01 M Tris-HCl buffer, pH 7.3, at 0.05 mg of total lipid/ml was incubated with SUV as the acceptor (80 mol% of egg PC and 20 mol% of cholesterol) at 0.5 mg total lipid/ml for 10 min at room temperature. SUV were made as described in ref. 37. The amount of recombinant rSCP2 present in the incubation medium (total volume = 1 ml) is plotted on the x-axis. After 10 min the donor and acceptor vesicles were separated by chromatography on DEAE Sepharose CL-6B, and the radioactivity present in the acceptor vesicles was determined in a Beckman LS 7500 scintillation counter. Pre-rSCP2 (■); mature rSCP2 (×).

between two populations of small unilamellar vesicles (SUV) carried out according to ref. 37. Figure 3 shows rates of cholesterol exchange as a function of added pre-rSCP2 and mature rSCP2. The exchange rates measured for pre-rSCP2 and mature rSCP2 were identical within experimental error. This finding is corroborated by kinetic measurements summarized in figure 4. The top curve represents passive exchange of cholesterol between two populations of SUV, i.e. cholesterol exchange in the absence of rSCP2. The addition of both pre-rSCP2 and mature rSCP2 accelerated the cholesterol exchange. The kinetic curves in figure 4 could be adequately fitted by a single exponential decay, and pseudo-first order rate constants k_1 and half times $t_{1/2}$ were derived from curve fitting. Passive exchange of cholesterol between two populations of SUV was characterized by $k_1 = 0.12$ h^{-1} ($t_{1/2} = 6$ h) (top curve, fig. 4). The k_1 and $t_{1/2}$ values obtained for equal concentrations of pre-rSCP2 and mature rSCP2 were identical within the error of the measurement, $k_1 = 0.035 \pm 0.009$ min^{-1} ($t_{1/2} = 20$ min) and $k_1 = 0.037 \pm 0.01$ min^{-1} ($t_{1/2} = 19$

min). At pre-rSCP2 concentrations of 20 mg protein/ml (1.5 mM) (bottom curve, fig. 4) the rate constant was increased to $k_1 = 0.11$ min^{-1} ($t_{1/2} = 6$ min). The results presented in figures 3 and 4 are consistent with data reported for rat pre-SCP2 [38, 39]. They clearly indicate that pre-SCP2 is active in lipid exchange, and cleavage of the 20-amino acid presequence has little if any effect on this activity.

Using the *E. coli* expression system it was possible to produce pre-rSCP2 in milligram quantities. However, because of the low solubility of pre-rSCP2 in aqueous solution, the maximum concentration obtainable was 0.3 mM. Since concentrations of 1.5 mM could be easily reached with mature rSCP2 and hSCP2 [6], the 20-amino acid presequence apparently reduces the solubility of SCP2 significantly. Thus the NMR experiments described below had to be carried out at protein concentrations ~0.3 mM.

Sequence-specific ^{15}N/^{1}H assignments and assignment of [^{1}H,^{1}H] NOEs. Out of 165 expected cross-peaks, 158 were observed in a 2D [^{15}N,^{1}H]-heteronuclear single-quantum coherence (HSQC) spectrum of pre-rSCP2 (fig. 5B), which was the starting point for the sequential resonance assignment. The ^{15}N and ^{1}H chemical shifts obtained were used to define the corresponding positions in a 3D ^{15}N-resolved [^{1}H,^{1}H]-TOCSY experiment
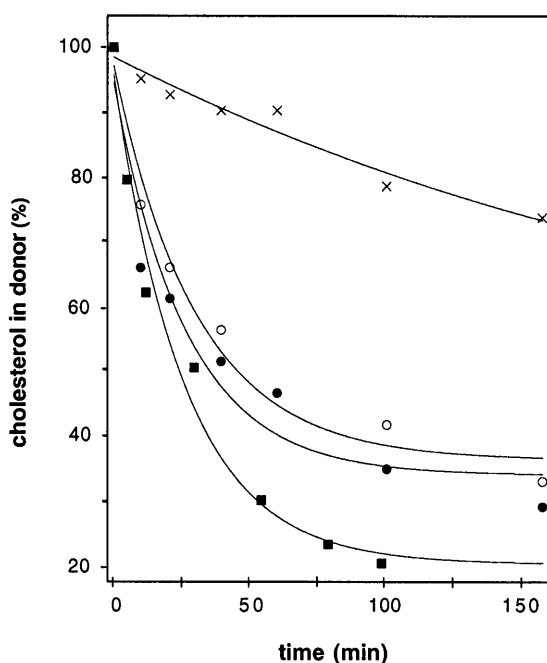

Figure 4. The kinetics of cholesterol exchange between two populations of SUV in the absence and presence of recombinant rSCP2. The experimental conditions were as described in the legend to figure 3. After timed intervals aliquots of the incubation medium were passed through a DEAE Sepharose CL-6B column to separate donor and acceptor vesicles, and the radioactivity present in the donor vesicles was determined. The kinetics of cholesterol exchange were measured in the absence of rSCP2 ($\times$), in the presence of 4 mg/ml pre-rSCP2 (0.26 μM) (○), 4 mg/ml mature rSCP2 (0.31 μM) (●), 20 mg/ml pre-rSCP2 (1.3 μM), (■).

Table 1. Comparison of long-range NOE distance constraints in pre-rSCP2 and hSCP2.

Proton I*	Proton II*	Distance (Å)	
		pre-rSCP2	hSCP2
V48 γ_1CH$_3$	S80 H^N	4.4	4.5
†V48 γ_2CH$_3$	N76 H^N		
V48 γ_2CH$_3$	K78 H^N	6.0	4.6
†V48 γ_2CH$_3$	G79 H^N		
I54 βCH	D90 H^N	3.1	3.1
I54 γ_2CH$_3$	D90 H^N	3.6	3.5
‡F55 HN	V72 HN	4.8	5.0
‡A56 HN	C91 HN	4.0	4.4
‡F57 H^N	W70 H^N	5.0	3.8
‡K58 αCH	W70 H^N	5.0	4.1
‡V59 H^N	A68 H^N	4.1	3.5
‡V59 αCH	I95 H^N	3.2	3.6
‡K60 H^N	I95 H^N	5.0	5.0
K60 H^N	D97 H^N	5.0	4.0
‡T69 αCH	V59 H^N	5.0	3.3
†T69 γ_2CH$_3$	S85 H^N	4.0	5.8
†‡V71 H^N	L82 H^N		
V71 γ_2CH$_3$	S85 H^N	6.0	5.8
‡D73 H^N	S80 H^N	3.8	3.5
D73 β_2CH	S80 H^N	5.0	4.2
‡V81 αCH	D73 H^N	2.8	3.8
A89 βCH$_3$	A56 H^N	3.8	3.4
‡T94 H^N	T122 H^N	4.8	4.5
A96 βCH$_3$	D99 H^N	3.4	3.4

*The residue numbering of pre-rSCP2 is used. †These NOE intensities could not be evaluated because of spectral overlap. ‡NOEs indicated in figure 8.

Figure 5. Contour plots of 2D [^{15}N,^{1}H]-HSQC spectra of uniformly ^{15}N-labelled hSCP2 (*A*) and pre-rSCP2 (*B*) recorded at a ^{1}H-frequency of 600 MHz in 90% H$_2$O/10% D$_2$O containing 15 mM KH$_2$PO$_4$ and 5 mM DTT at pH 6.0 and 28 °C, and sample concentrations of 1.3 and 0.3 mM, respectively. In (*B*) the cross-peaks identified with the amino acid number were assigned using 3D ^{15}N-resolved [^{1}H,^{1}H]-TOCSY and [^{1}H,^{1}H]-NOESY spectra. For the resonance assignments of hSCP2 in (*A*) see figure 2 in ref. [6]. The chemical shifts are relative to 2,2-dimethyl-2-silapentane-5-sulphonate sodium salt.

[31, 32]. Using the peak positions of the 3D ^{15}N-resolved [^{1}H,^{1}H]-TOCSY spectrum, 198 intraresidual NOE connectivities, and 58 d_{NN}, 62 $d_{\alpha N}$ and 25 $d_{\beta N}$ sequential NOE connectivities were identified in a 3D ^{15}N-resolved [^{1}H,^{1}H]-NOESY spectrum. On this basis, sequence-specific assignments were obtained for 105 out of the 143 residues. In addition, we assigned 25 medium-range and long-range backbone-backbone NOEs, and 13 interresidual NOEs involving side-chain protons (table 1 and fig. 7). For the N-terminal leader sequence of pre-rSCP2, no sequence-specific assignments could be established because of scarcity of sequential NOEs [40], which is probably due to both the low protein concentration and conformational exchange with concomitant line broadening.

Chemical shift differences between corresponding residues in rabbit pre-rSCP2 and hSCP2. Figure 6 displays the differences of the ^{15}N and ^{1}H chemical shifts between corresponding residues of rabbit pre-rSCP2 and hSCP2 [6]. The small mean chemical shift differences of backbone ^{15}N and ^{1}H nuclei of 0.16 ppm and 0.01 ppm, respectively, strongly suggest that the residues 20–143 of pre-rSCP2 form the same 3D fold as hSCP2 [6]. Larger chemical shift differences were observed for three out of the four amino acid residues that are different in hSCP2 and pre-rSCP2, i.e. Gly24, Leu100

Figure 6. Plots of backbone ^{15}N (solid line) and ^{1}H (dotted line) chemical shift differences between hSCP2 [6] and pre-rSCP2. Asterisks indicate the four positions with different amino acids in hSCP2 [6] and pre-rSCP2: Gly 24 (pre-rSCP2) → Ser 4 (hSCP2), Ile 95 (pre-rSCP2) → Met75 (hSCP2), Leu100 (pre-rSCP2) → Phe80 (hSCP2), and Lys140 (pre-rSCP2) → Asn120 (hSCP2).
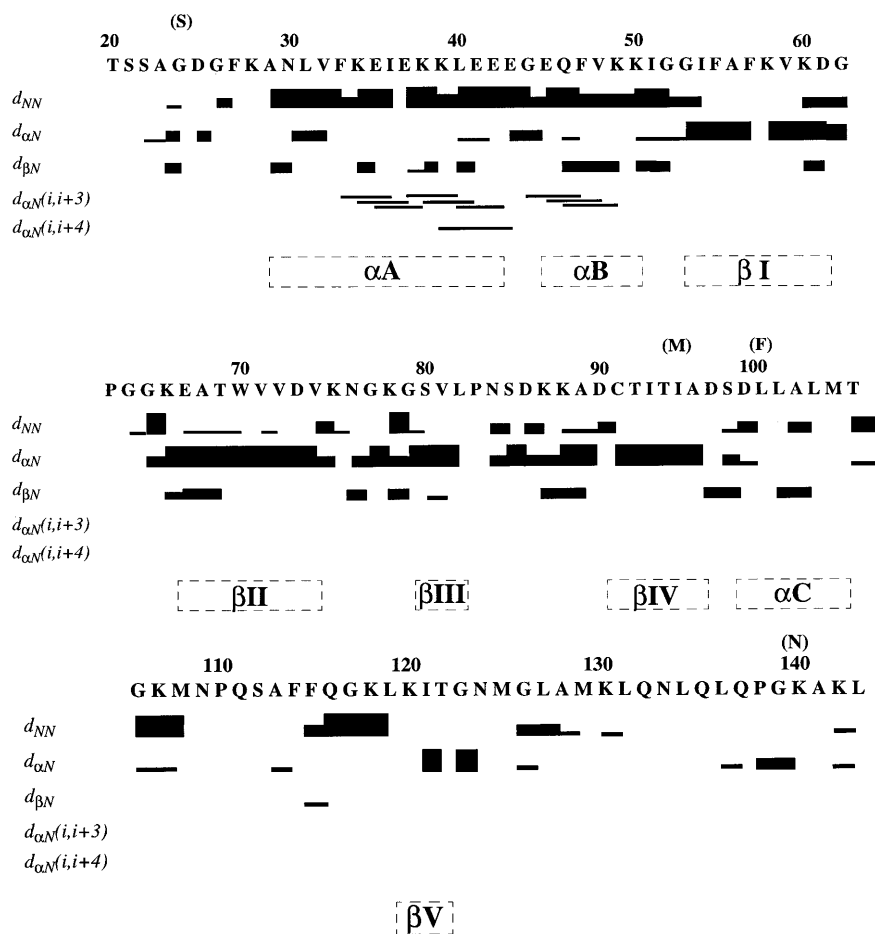
Figure 7. Sequential and medium-range NOE connectivities observed for the polypeptide segment 20–143 of pre-rSCP2. The thickness of the bars for the sequential connectivities represents the NOE intensities. The sequence location of the regular secondary structure elements identified for hSCP2 [6] are represented by dashed boxes. Above the amino acid sequence of pre-rSCP2, the four residues that are different in hSCP2 are indicated in parentheses.

and Lys140 in pre-rSCP2, corresponding to Ser4, Phe80 and Asn120 in hSCP2. These changes are due to the different amino acids [40, 41] and do not reflect 3D structure differences.

Secondary structure of pre-rSCP2. Overall, the analysis of the 3D ^{15}N-resolved [^{1}H,^{1}H]-NOESY spectrum of pre-rSCP2 yielded the identification of 378 NOEs. Based on the sequential and medium-range NOE connectivities (fig. 7) and on comparison of the relative peak intensities of the sequential NOEs with those observed in a 3D ^{15}N-resolved [^{1}H,^{1}H]-NOESY spectrum of hSCP2 [6], we identified regular secondary structure elements present in pre-rSCP2. Helices were identified due to the presence of strong d_{NN} sequential NOEs and diagnostic medium-range $d_{\alpha N}(i,i+3)$ and $d_{\alpha N}(i,i+4)$ NOEs, and the β strands were derived from the presence of strong $d_{\alpha N}$ NOEs and concomitantly

weak d_{NN} NOEs [42]. Two helices and four β strands could thus be identified in pre-rSCP2, which correspond to αA, αB, βI, βII, βIII and βIV in hSCP2. The presence in pre-rSCP2 of the complete +1, +1, +3x, −1 β sheet that was previously also found in mature hSCP2 is supported by the observation of interstrand NOEs, which also implicate the presence of the fifth β-strand (fig. 8).

3D polypeptide fold. For the polypeptide segment 20–143 in pre-rSCP2 and hSCP2 [6], near-identity of the backbone ^{15}N and ^{1}H chemical shifts, similar ^{15}N and ^{1}H resonance line widths, coincidence of regular secondary structures (figs 7 and 8) and the identification of 24 corresponding long-range [^{1}H,^{1}H] NOEs in the two proteins provide evidence for very similar 3D folds and dimeric states. In view of the high sequence identity (97%) this is not unexpected, but it was not a priori
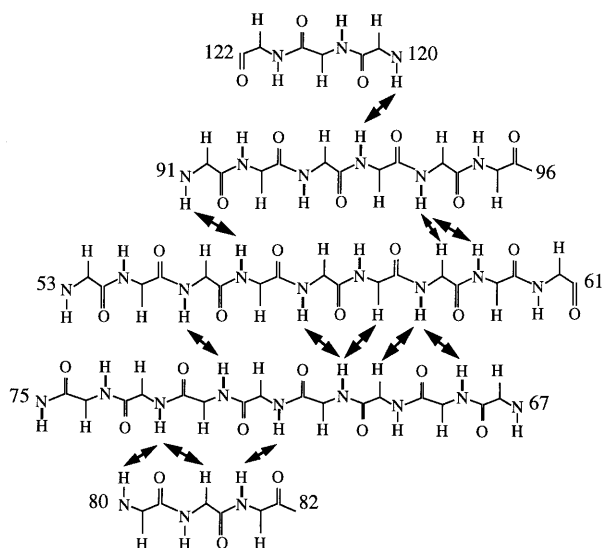
Figure 8. The five-stranded β-sheet found in *h*SCP2 [6] with the amino acid sequence numbering of pre-*r*SCP2 (fig. 1). Interstrand NOEs that were observed in a 3D ^{15}N-resolved [^{1}H,^{1}H]-NOESY spectrum of pre-*r*SCP2 are indicated by double-headed arrows.

clear whether the additional leader sequence in pre-*r*SCP2 would significantly perturb the 3D fold. The finding that pre-*r*SCP2 and mature *h*SCP2 fold to the same structure type is entirely consistent with the observation that both proteins have similar activities. It also contributes to rationalizing the fact that previous studies did not show differences between pre-SCP2 and mature SCP2 in their abilities to stimulate microsomal conversion of 7-dehydrocholesterol to cholesterol, and to transfer cholesterol and phosphatidylcholine from donor SUV to acceptor membranes [14].

For the N-terminal 20-residue leader sequence, the 18 cross-peaks expected in the 2D [^{15}N,^{1}H]-correlation spectroscopy (COSY) spectrum could be identified by comparison with the corresponding spectrum recorded for mature *h*SCP2 (fig. 5). However, we could not obtain sequence-specific resonance assignments because only very few cross-peaks could be detected in 3D ^{15}N-resolved [^{1}H,^{1}H]-NOESY spectra. Cross-peaks in 3D ^{15}N-resolved [^{1}H,^{1}H]-TOCSY spectra were observed only for eight residues. These observations would be compatible with the assumption that the 10 residues of the leader sequence, which are unobservable in both NOESY and TOCSY, are subject to line broadening by conformational exchange processes on the millisecond time scale. This indicates that the leader sequence in the solution structure of pre-*r*SCP2 has some nonrandom conformational properties. Interestingly, a secondary structure prediction using the program PHDsec [43]

yielded an α-helical polypeptide segment comprising residues 6 to 14 of pre-*r*SCP2. It might thus be that the putative conformational exchange processes evidenced by the broadened NMR signals are helix-coil transitions, so that an α-helical conformation is adopted only transiently in parts of the leader peptide.

The functional role of pre-SCP2 remains unclear. Apparently, cleavage of the presequence does not confer lipid exchange activity upon SCP2, because preform and mature form of SCP2 have similar activities. The presequence has similarity to known mitochondrial targeting sequences [39], but its possible role as a targeting signal has yet to be subjected to experimental test.

1 Bloj B. and Zilversmit D. B. (1977) Accelerated transfer of neutral glyco-sphingolipids and ganglioside GM 1 by a purified lipid transfer protein. J. Biol. Chem. **252:** 1613–1619

2 Seedorf U. and Assmann G. (1991) Cloning, expression and nucleotide sequence of rat liver sterol carrier protein 2 cDNAs J. Biol. Chem. **266:** 630–636

3 Yamamoto R., Kallen C. B., Babalola G. O., Rennert H., Billheimer J. T. and Strauss J. F. (1991) Cloning and expression of a cDNA encoding human sterol carrier protein 2. Proc. Natl. Acad. Sci. USA **88:** 463–467

4 Moncecchi D., Pastuszyn A. and Scallen T. J. (1991) cDNA sequence and bacterial expression of mouse liver sterol carrier protein 2. J. Biol. Chem. **266:** 9885–9892

5 Pfeifer S. M., Sakuragi N., Ryan A., Alan L., Johnson R. G. D., Billheimer J. T. et al. (1993) Chicken sterol carrier protein2/ sterol carrier protein X: cDNA cloning reveals evolutionary conservation of structure and regulated expression. Arch. Biochem. Biophys. **304:** 287–293

6 Szyperski T., Scheek S., Johansson J., Assmann G., Seedorf U. and Wüthrich K. (1993) NMR determination of the secondary structure and the three-dimensional polypeptide backbone fold of the human sterol carrier protein 2. FEBS Lett. **335:** 18–26

7 Noland B. J., Arebalo R. E., Hansbury E. and Scallen T. J. (1980) Purification and properties of sterol carrier protein-2. J. Biol. Chem. **255:** 4282–4289

8 Trzaskos J. M. and Gaylor J. L. (1983) Cytosolic modulators of activities of microsomal enzymes of cholesterol biosynthesis. Purification and characterization of a non-specific lipid-transfer protein. Biochim. Biophys. Acta **751:** 52–65

9 Seltman H., Diven W., Rizk M. and Noland B. J. (1985) Regulation of bile-acid synthesis. Role of sterol carrier protein 2 in the biosynthesis of 7 alpha-hydroxycholesterol. Biochem. J. **230:** 19–24

10 Chanderbhan R., Noland B. J., Scallen T. J. and Vahouny G. V. (1982) Sterol carrier protein 2. Delivery of cholesterol from adrenal lipid droplets to mitochondria for pregnenolone sythesis. J. Biol. Chem. **257:** 8928–8934

11 McNamara F. C. and Jefcoate C. R. (1989). The role of sterol carrier protein in stimulation of steroidogenesis in rat adrenal mitochondria by adrenal cytosol. Arch. Biochem. Biophys. **275:** 53–62

12 Van Noort M., Focko F. G., Van Amerongen A. and Wirtz K. W. A. (1988) Intracellular redistribution of SCP-2 in Leydig

cells after hormonal stimulation may contribute to increased pregnenolone production. Biochem. Biophys. Res. Commun. **154:** 60–65

13 Frolov A., Cho T.-H., Billheimer J. T. and Schroeder F. (1996) Sterol carrier protein-2, a new fatty acyl coenzyme A-binding protein J. Biol. Chem. **271:** 31878–31884

14 Seedorf U., Scheek S., Engel T., Steif C., Hinz H.-J. and Assmann G. (1994) Structure activity studies of human sterol carrier protein 2. J. Biol. Chem. **269:** 2613–2618

15 Baum C. L., Reschly E. J., Gayen A. K., Groh M. E. and Schadick K. (1997) Sterol carrier protein-2 overexpression enhances sterol cycling and inhibits cholesterol ester synthesis and high density lipoprotein cholesterol secretion. J. Biol. Chem. **272:** 6490–6498

16 Puglielli L., Rigotti A., Amigo L., Nunez L. Greco A. V., Santos M. J. et al. (1996) Modulation of intrahepatic cholesterol trafficking: evidence by in vivo antisense treatment for the involvement of sterol carrier protein-2 in newly synthesized cholesterol transport into rat bile. Biochem. J. **317:** 681–687

17 Gould S. J., Keller G. A., Hosken W., Weilkenson J. and Subramani S. (1989) A conserved tripeptide sorts proteins to peroxisomes. J. Cell Biol. **108:** 1657–669

18 Keller G. A., Scallen T. J., Clarke D., Maher P. A., Krisans S. K. and Singer S. J. (1989) Subcellular localization of sterol carrier protein-2 in rat hepatocytes: its primary localization to peroxisomes. J. Cell Biol. **108:** 1353–1361

19 Van Heusden G. P. H., Bos K., Raetz C. R. H. and Wirtz K. W. A. (1990) The occurrence of souble and membrane-bound non-specific lipid transfer protein (sterol carrier protein 2) in rat tissues. J. Biol. Chem. **265:** 4105–4110

20 Wouters F. S., Markman M., deGraaf P., Hauser H., Tabak H. F., Wirtz K. W. A. et al. (1995) The immunohistochemical localization of the non-specific lipid transfer protein (sterol carrier protein 2) in rat small intestine enterocytes. Biochim. Biophys. Acta **1259:** 192–196

21 Nicholson D. W. and Neupert W. (1988) Synthesis and assembly of mitochondrial proteins. In: Protein Transfer and Organelle Biogenesis, pp. 677–729, Das R. C. and Robbins P. N. (eds), Academic Press, Boston

22 Moncecchi D., Murphy E. J., Prows D. R. and Schroeder F. (1996) Sterol carrier protein-2 expression in mouse L-cell fibroblasts alters cholesterol uptake. Biochim. Biophys. Acta **1302:** 110–116

23 Murphy E. J. and Schroeder F. (1997) Sterol carrier protein-2 mediated cholesterol esterification in transfected L-cell fibroblasts. Biochim. Biophys. Acta **1345:** 283–292

24 Van Heusden G. P. H., Bos K. and Wirtz K. W. A. (1990) The occurrence of souble and membrane-bound non-specific lipid transfer protein (sterol carrier protein 2) in rat tissues. Biochim. Biophys. Acta **1046:** 315–21

25 Lipka G., Schulthess G., Thurnhofer H., Wacker H., Wehrli E., Zeman K. et al. (1995) Characterization of lipid exchange proteins isolated from small-intestinal brush border membrane. J. Biol. Chem. **270:** 5917–5925

26 Sambrook J., Fritsch E. F. and Maniatis T. (1989) Molecular Cloning: A Laboratory Manual, 2nd ed., Cold Spring Harbor Laboratory Press, Plainview, NY

27 Marion D., Ikura K., Tschudin R. and Bax A. (1989) Rapid recording of 2D spectra without phase cycling: application of the study of hydrogen exchange proteins. J. Magn. Reson. **85:** 393–399

28 Güntert P., Dötsch V., Wider G. and Wüthrich K. (1992) Processing of the multidimensional NMR data with the new software PROSA. J. Biomol. NMR **2:** 619–629

29 Bartels C., Xia T., Billeter M., Güntert P. and Wüthrich K. (1995) The program XEASY for computer-supported NMR spectral analysis of biological macromolecules. J. Biomol. NMR **6:** 1–10

30 Bodenhausen G. and Ruben D. (1980) Natural abundance ^{15}N NMR by enhanced heteronuclear spectroscopy. Chem. Phys. Lett. **69:** 185–188

31 Fesik S. W. and Zuiderweg E. R. P. (1988) Heteronuclear three-dimensional NMR spectroscopy. A strategy for the simplification of homonuclear two-dimensional NMR spectra. J. Magn. Reson. **78:** 588–593

32 Marion D., Kay L. E., Sparks S. W., Torchia D. A. and Bax A. (1989) Three-dimensional heteronuclear NMR of ^{15}N-labelled proteins. J. Am. Chem. Soc. **111:** 1515–1517

33 Messerle B. A., Wider G., Otting G., Weber C. and Wüthrich K. (1989) Solvent suppression using a spin lock in 2D and 3D NMR spectroscopy with H$_2$O solutions. J. Magn. Reson. **85:** 608–613

34 Marion D., Ikura K. and Bax A. (1989) Improved solvent suppression in one- and two-dimensional NMR spectra by convolution of time-domain data. J. Magn. Reson. **84:** 425–430

35 DeMarco A. and Wüthrich K. (1976) Digital filtering with a sinusoidal window function: an alternative technique for resolution enhancement in FT NMR. J. Magn. Reson. **24:** 201–204

36 Güntert P. and Wüthrich K. (1992) FLATT: a new procedure for high-quality baseline correction of multidimensional NMR spectroscopy. J. Magn. Reson. **96:** 403–407

37 Schulthess G., Lipka G., Compassi S., Boffelli D., Weber F. E., Paltauf F. et al. (1994) Absorptions of monoacylglycerols by small-intestinal brush border membrane. Biochemistry **33:** 4500–4508

38 Ossendorp B. C., Geijtenbeek T. B. H. and Wirtz K. W. A. (1992) The occurrence of souble and membrane-bound non-specific lipid transfer protein (sterol carrier protein 2) in rat tissues. FEBS Lett. **296:** 179–183

39 Matsuura J. E., George H. J., Ramachandran N., Alvarez J. G., Strauss J. F. III and Billheimer J. T. (1993) Expression of the mature and the pro-form of human sterol carrier protein 2 in *Escherichia coli* alters bacterial lipids. Biochemistry **32:** 567–572

40 Wüthrich K. (1986) NMR of proteins and nucleic acids. In: NMR of Proteins and Nucleic Acids, Wiley, New York

41 Braun D., Wider G. and Wüthrich K. (1994) Sequence-correction ^{15}N 'Random Coil' chemical shifts. J. Am. Chem. Soc. **116:** 8466–8469

42 Wüthrich K., Billeter M. and Braun W. (1984) Pseudo-structures for the 20 common amino acids for use in studies of protein conformations by measurements of intramolecular proton-proton distance constraints with nuclear magnetic resonance. J. Mol. Biol. **180:** 715–740

43 Rost B. and Sander C. (1994) Conservation and prediction of solvent accessibility in protein families. Proteins **19:** 55–72